High-Resolution Direction Finding of Non-stationary Signals Using Matching Pursuit

Sedigheh Ghofrani[1], Moeness G. Amin[2], and Yimin D. Zhang[2]

[1] Electrical Engineering Department, Islamic Azad University, Tehran South Branch, Tehran, IRAN

[2] Center for Advanced Communications, Villanova University, Villanova, PA 19085, USA

e-mails: s_ghofrani@azad.ac.ir, moeness.amin@villanova.edu, yimin.zhang@villanova.edu

Abstract: One of the main goals of time-frequency (TF) signal representations in non-stationary array processing is to equip multi-antenna receivers with the ability to separate sources in the TF domain prior to direction finding. This permits high-resolution direction-of-arrival (DOA) estimation of individual sources and of more sources than sensors. In this paper, we use linear decomposition of sensor data based on matching pursuit (MP). The leading atoms of the MP, which capture most of the source TF signatures, can be different for different sources and, as such, provide the desired source discrimination. The MP coefficients with high signal-to-noise ratio (SNR) and corresponding to the leading decomposition atoms are used to develop the MP-MUSIC DOA estimation for non-stationary source signals. We demonstrate the source discriminatory capability of the proposed technique using linear FM, nonlinear FM, and other non-stationary signals. Further, we compare MP-MUSIC performance with conventional MUSIC and the time-frequency MUSIC, which incorporates bilinear transforms.

1. INTRODUCTION

High-resolution direction finding of non-stationary signals can exploit the time-frequency (TF) signatures of the sources in the field of view to provide source discrimination and increased signal-to-noise ratio (SNR) [1]. Both capabilities have been achieved within the spatial time-frequency distribution (STFD) framework. This framework was applied to narrowband signals in [2]-[3] and extended to wideband sources by Gershman et al. in [4]-[6]. The STFD framework applies a form of joint-variable signal representations to expose hidden TF signatures characterizing the data received by the antenna array. Signal analysis in a single domain, whether time or frequency, fails to reveal the local behavior of the signal and in expressing its power distribution over both time and frequency. On the other hand, bilinear transforms, such as Cohen's class [7] of time-frequency distributions (TFD), capture the instantaneous frequency (IF) laws underlying the non-stationarity of the data.

The STFD matrix, in lieu of the covariance matrix, permits the auto- and cross-TFDs of the sensor data to retain the signal phase and, as such, embeds the sources' direction-of-arrival (DOA) information. DOA estimation approaches using subspace methods, such as MUSIC [8], and incorporating the STFDs have been shown to improve the performance over their covariance matrix counterparts, primarily because of their capability to successfully discriminate among sources and exclude some from consideration prior to subspace decomposition. Accordingly, the STFD-based DOA approaches become attractive for sources with close angular separations, but with distinctive IFs [9].

In this paper, we provide an alternative to the STFD framework which enjoys the same benefits of STFDs. We use linear, in lieu of quadratic, TF signal representations by employing matching pursuit (MP) [10] in which the decomposition coefficients bear the source TF localization profiles. These coefficients act like the signal auto-terms in bilinear TF transforms. However, unlike the bilinear STFD approach, where the cross-sensor distribution is needed to capture the phase changes across the array, the linear decomposition of the data at each sensor using MP preserves the signal phase. The MP-MUSIC is developed by forming the coefficient covariance matrix and then applying eigen-decomposition for subspace estimation.

MP is an adaptive signal decomposition technique that is energy conservative. While first introduced by using the Gabor functions as atoms, MP has been extended to use dictionaries consisting of any Gaussian envelopes with arbitrary phase laws (e.g., constant, linear, cubic and polynomial). Clearly, using atoms with more parameters provides higher flexibility in matching the signals, but also increases the computational cost. From DOA estimation

perspective, MP offers the same key advantages of STFD, i.e., source discrimination and SNR enhancement. It is applicable to a broad class of non-stationary signals, not necessarily those characterized by their IFs. Further, unlike the STFD, where TF points or regions of high power concentrations need to be identified post distribution computations through thresholding, MP automatically and chronologically identifies atoms that capture these regions according to their energy contributions. This directly determines the best TF regions to be incorporated in DOA estimation.

MP was used to estimate the source DOA in a manner similar to the maximum likelihood (ML) method in [11]-[13]. In these approaches, DOA estimation is performed by utilizing a large dictionary that includes steering vectors for all possible signal arrivals. Although the algorithm converges over few snapshots, the computational cost is rather considerable. This procedure of applying MP for steering vectors is entirely different from the one proposed in this paper, where the source non-stationarity is addressed by the MP decomposition in the temporal domain, followed by subspace decomposition of the MP coefficient covariance matrix for DOA estimation. Linear TF decompositions, using the wavelet transform, have been used for de-noising prior to DOA estimation in [14]-[17]. In contrast to the wavelet approach, the proposed approach incorporates the MP into DOA and uses the decomposition coefficients directly into signal and noise subspace decompositions.

In this paper, we develop high-resolution DOA estimation techniques of non-stationary narrowband signals using MP, and demonstrate the proposed technique's source discriminatory capability and its robustness against noise. A priori knowledge of the coarse source TF behavior, if available, can aid in tailoring the atoms to a specific problem. This knowledge can be gained, e.g., from the TFD of the reference sensor or from the averaged TFDs across the sensor array (e.g., [18]). In the absence of this knowledge, the chirplet atoms can be adopted because of their attractive TF concentration properties [19]-[22]. When proper matching of atoms and signals occurs, each of the leading atoms captures one signal, allowing DOA estimation of a single source to be performed for each atom. The consequence of using a general set of atoms, like chirplets, in the absence of *a priori* information of the signals is two-fold. First, more atoms are required to properly decompose the signals and capture their energy. Second, some atoms may overlap with two or more sources. These atoms assume a similar role of cross-terms in the STFD framework and may hinder source discrimination. In both cases, an association procedure is performed to attempt to group the atoms and the coefficients [23].

This paper is organized as follows. In Section 2, we introduce the signal model, and review the conventional MUSIC technique as well as the STFD concept. A short overview of the MP decomposition is provided in Section 3. In Section 4, we develop MP-MUSIC for DOA estimations. It is shown that the MP coefficient covariance matrix can be used as an alternative to the spatial covariance and STFD matrices to formulate subspace-based DOA estimation methods within the MP framework. The MP-MUSIC performance is provided in Section 5. Section 6 presents simulation results, and finally Section 7 concludes this paper.

The following notations are used in this paper. Boldface lower-case letters (e.g., $\mathbf{a}$) denote vectors, and boldface upper-case letters (e.g., $\mathbf{A}$) denote matrices. $\mathrm{E}[.]$ represents the statistical mean operation. $(.)^{*}$, $(.)^{T}$ and $(.)^{H}$ denote complex conjugate, transpose and conjugate transpose, respectively. $\delta(.)$ denotes the Kronecker delta function, and $\mathbf{I}$ is an identity matrix. In addition, $C^{M \times N}$ denotes the space of $M \times N$ matrices with complex entries. $< \mathbf{a}, \mathbf{b} >= \mathbf{a}^{T}\mathbf{b}^{*}$ denotes the inner product of two vectors $\mathbf{a}$ and $\mathbf{b}$, and $\|.\|$ denotes the Frobenius norm of a vector.

2. SIGNAL MODEL

In this section, we introduce the signal model. For the convenience of presentation, we briefly review the MUSIC and the STFD concept [1, 8].

2.1. Signal Model

Assume K non-coherent narrow-band signal sources impinging on an M-element with angles θ_k, $k=1, 2,...,K$. The array output vector at time instant t, $\mathbf{x}(t)=[x_1(t), x_2(t),...,x_M(t)]^{T}$, is expressed as

$$\mathbf{x}(t)=\mathbf{As}(t)+\mathbf{n}(t), \quad t=1,2,...,N \tag{1}$$

where N is the number of snapshots, $\mathbf{s}(t)=[s_1(t), s_2(t),...,s_K(t)]^{T}$ is the source signal vector, and $\mathbf{n}(t)=[n_1(t), n_2(t),...,n_M(t)]^{T}$ is an additive noise vector whose elements are modeled as stationary, spatially and temporally white Gaussian, zero-mean complex random processes, independent of the source signals, i.e., $\mathrm{E}[\mathbf{n}(t+\tau)\mathbf{n}^{H}(t)]=\sigma_n^2\delta(\tau)\mathbf{I}$, with σ_n^2 denoting the variance. In particular, when the array is uniform linear, then the k-th column of the steering matrix $\mathbf{A}=[\mathbf{a}(\theta_1),\mathbf{a}(\theta_2),...,\mathbf{a}(\theta_K)]$ is expressed as $\mathbf{a}(\theta_k)=[1,e^{j\omega_k},...,e^{j(M-1)\omega_k}]^{T}$, where

$\omega_k = 2\pi \dfrac{d}{\lambda} \sin(\theta_k)$ is the spatial frequency of the k-th signal, λ denotes the wavelength, and d is the inter-element

spacing.

The spatial covariance matrix of $\mathbf{x}(t)$ is defined as

$$\mathbf{C}_{\mathbf{xx}} = \mathrm{E}[\mathbf{x}(t)\mathbf{x}^H(t)] = \mathbf{A}\mathbf{C}_{\mathbf{ss}}\mathbf{A}^H + \sigma_n^2\mathbf{I}, \tag{2}$$

where $\mathbf{C}_{\mathbf{ss}} = \mathrm{E}[\mathbf{s}(t)\mathbf{s}^H(t)]$ is the source covariance matrix. In practice, the true covariance matrix $\mathbf{C}_{\mathbf{xx}}$ is unknown,

and is estimated from the available data samples as $\hat{\mathbf{C}}_{\mathbf{xx}} = \sum_{t=1}^{N} \mathbf{x}(t)\mathbf{x}^H(t)/N$.

2.2 MUSIC Algorithm

Assume that the number of sources is less than the number of sensors. The MUSIC algorithm estimates the source

DOAs by finding the peaks of the following spatial pseudo-spectrum, i.e., the reciprocal of the projection of the

search steering vector to the noise subspace estimate, $\hat{\mathbf{E}}_{\mathbf{n}}$,

$$P(\theta) = \frac{1}{\mathbf{a}^H(\theta)\hat{\mathbf{E}}_{\mathbf{n}}\hat{\mathbf{E}}_{\mathbf{n}}^H\mathbf{a}(\theta)}. \tag{3}$$

2.3. STFD

The class of all quadratic, shift invariant, TFDs is known as the Cohen's class [7]. In particular, the Wigner-Ville

distribution (WVD) is the simplest member of the Cohen's class, represented as

$$\mathbf{W}_{xx}(t, f) = \int_{-\infty}^{+\infty} x(t + \frac{\tau}{2}) x^*(t - \frac{\tau}{2}) e^{-j2\pi f\tau} d\tau. \tag{4}$$

The WVD is known to provide the best resolution for linear frequency modulated (LFM) signals among the Cohen's

class, but it generates cross-term interference when analyzing multi-component signals or for signals with nonlinear

frequency characteristics. It is important to note that the former cross-term is referred to as the inner-interference,

whereas the latter is outer-interference.

Under the linear data model, Eq. (1), the STFD matrix can be defined for any Cohen's class of TFDs [1], [24].

For WVD, the statistical expectation of the STFD matrix of $\mathbf{x}(t)$, $\mathbf{W}_{\mathbf{xx}}(t,f) \in C^{M \times M}$, is expressed as,

$$\mathrm{E}[\mathbf{W}_{\mathbf{xx}}(t,f)] = \mathbf{A}\mathrm{E}[\mathbf{W}_{\mathbf{ss}}(t,f)]\mathbf{A}^H + \sigma_n^2\mathbf{I}, \tag{5}$$

where $\mathbf{W}_{ss}(t,f) \in C^{K \times K}$ is the signal TFD matrix whose entries are the auto- and cross-source WVDs. We note that $\mathrm{E}[\mathbf{W}_{xx}(t,f)]$ can be constructed for any selected TF points or TF regions. The spatially averaged TFD matrix was proposed in [25]-[26] to reduce noise and cross-terms contributions. The main difficulty of the STFD-based approaches is two-fold: First, they need to identify, and then use, high power signal concentration regions in the TF domain; Second, they assume clear IF characterization of the source signals. This difficulty can be avoided when MP, in lieu of the STFD, is used as discussed below.

3. MP DECOMPOSITION

In this section, we first review the MP signal decomposition theory for noise-free signals and then consider the MP adaptive decomposition when the signals are corrupted by additive noise.

3.1 MP Decompositions

The MP adaptive signal decomposition is based on a dictionary that contains a family of functions called elementary functions or TF atoms [10]. Let H be a Hilbert space, and $D = \{\mathbf{g}_l\}$ as a redundant dictionary including a family of functions in H, each is normalized to unit norm, i.e. $\| \mathbf{g}_l \| = 1$, and t refers to discrete time. MP decomposes a signal, $\mathbf{x} = [x(1),...,x(N)]^T \in H$, as a linear combination of atoms selected from D. The decomposition is performed by projecting the signal over the function dictionary and selecting the atoms which best match the local structure of the signal or have the highest correlation with the signal. After L iterations, the MP decomposition of an arbitrary signal $\mathbf{x}$ can be written as,

$$\mathbf{x} = \sum_{l=0}^{L-1} \widetilde{c}_l \mathbf{g}_l + \mathbf{x}^{[L]} , \tag{6}$$

where $\mathbf{x}^{[L]}$ denotes the residue after L times of signal decomposition, $\mathbf{g}_l$ is the chosen atom in the l-th iteration, and

$$\widetilde{c}_l = <\mathbf{x}^{[l]}, \mathbf{g}_l> \tag{7}$$

is the complex coefficient. We define $\mathbf{x}^{[0]} = \mathbf{x}$. As such, the MP algorithm decomposes the residue at each stage. It was shown in [10] that, when $\mathbf{x}$ is noise-free, the MP recovers its components, i.e.,

$$\mathbf{x} = \sum_{l=0}^{+\infty} \widetilde{c}_l \mathbf{g}_l , \tag{8}$$

provided that the dictionary is complete. In this case, the MP decomposition is also energy conservative, i.e.,

$$\| \mathbf{x} \|^2 = \sum_{l=0}^{+\infty} | \tilde{c}_l |^2 .$$

(9)

Since the equality in equation (8) applies to all signal samples, $t = 1, 2, ..., N$, it can be written as

$$x(t) = \sum_{l=0}^{+\infty} \tilde{c}_l \, g_l(t).$$

(10)

The WVD of the decomposed signal is,

$$W_x(t,f) = \sum_{l=0}^{+\infty} | \tilde{c}_l |^2 \, W_{g_l}(t,f) + \sum_{l=0}^{+\infty} \sum_{\substack{l'=0 \\ l \neq l'}}^{+\infty} \tilde{c}_l \tilde{c}_{l'}^* W_{g_l g_{l'}}(t,f),$$

(11)

were the double sum corresponds to the cross-terms of the WVD. Therefore, the MP distribution is defined by keeping the first term in the above expression [10],

$$E_x(t,f) = \sum_{l=0}^{+\infty} | \tilde{c}_l |^2 \, W_{g_l}(t,f).$$

(12)

3.2 MP Atoms

TF atoms can be expressed in a general expression, $g(t) = \dfrac{1}{\sqrt{s}} \gamma(\dfrac{t-u}{s}) e^{j\phi(t)}$, where $\gamma(t) = 2^{1/4} e^{-\pi t^2}$ denotes the

Gaussian envelope and $\phi(t)$ is an arbitrary phase law. Although MP was first introduced using the Gabor dictionary

[10], where $\phi(t) = \zeta t$, it has been extended to other dictionaries, such as the chirplet dictionary [27]-[29], where

$\phi(t) = \zeta t + \dfrac{\beta}{2} t^2$, and cubic dictionary [30], where $\phi(t) = \zeta t + \dfrac{\beta}{2} t^2 + \dfrac{\xi^3}{3} t^3$. In general, any Gaussian envelope with

an arbitrary phase law (e.g., constant, linear, cubic and high-order polynomial phase) can be used as TF atoms,

provided that the unit-norm requirement is satisfied. In particular, the Gabor and chirplet atoms are unique in the

sense that, among all atoms with Gaussian shape envelope, they have the highest concentration in both the time and

frequency domains [31]. In the cubic directory, the elements of the parameter set $(s, u, \zeta, \beta, \xi)$ are real and denote,

respectively, the width, the time center, the frequency center, the frequency modulation rate, and the frequency

curvature. In addition, the width, s, is always positive. Generally, there is no analytical solution to find the optimum

values of MP atoms parameters. As a result, there is a trade-off between flexibility in matching the signal and the

computational cost.

7

4. MP MODEL FOR DOA ESTIMATION

Consider a single source. Without loss of generality, we assume the reference sensor output, $x_1(t)$, but drop the subscript to simplify notation. The data observation vector at the reference sensor for N snapshots is expressed by,

$$\mathbf{x} = \mathbf{s} + \mathbf{n}.$$ (13)

We define $\mu_{l,l'} = <\mathbf{g}_{l'}, \mathbf{g}_l> \in [0,1]$ as the atom inner product or atom cross-correlation, $c_l = <\mathbf{s}, \mathbf{g}_l>$ as the signal decomposition coefficient, and $n_l = <\mathbf{n}, \mathbf{g}_l>$ as noise decomposition coefficient. For more details about the statistics of the noise decomposition coefficient, n_l, see appendix A.

At the first iteration, suppose atom $\mathbf{g}_0$ is the leading atom that has the highest correlation with the signal

$$<\mathbf{x}^{[0]}, \mathbf{g}_0> = c_0 + n_0.$$ (14)

Define $\tilde{c}_0 = c_0$; $\tilde{n}_0 = n_0$, then

$$\mathbf{x} = \tilde{c}_0 \mathbf{g}_0 + \tilde{n}_0 \mathbf{g}_0 + \mathbf{x}^{[1]}.$$ (15)

At the second iteration, suppose atom $\mathbf{g}_1$ has the highest correlation with the residual, $\mathbf{x}^{[1]}$, then it can be readily shown that

$$<\mathbf{x}^{[1]}, \mathbf{g}_1> = c_1 - \tilde{c}_0 \mu_{1,0} + n_1 - \tilde{n}_0 \mu_{1,0}.$$ (16)

Define $\tilde{c}_1 = c_1 - \mu_{1,0} \tilde{c}_0$, and $\tilde{n}_1 = n_1 - \mu_{1,0} \tilde{n}_0$, then

$$\mathbf{x} = \tilde{c}_0 \mathbf{g}_0 + \tilde{c}_1 \mathbf{g}_1 + \tilde{n}_0 \mathbf{g}_0 + \tilde{n}_1 \mathbf{g}_1 + \mathbf{x}^{[2]}.$$ (17)

Following the same procedure, and define $\tilde{c}_l = c_l - \sum_{i=0}^{l-1} \mu_{l,i} \tilde{c}_i$ as MP signal coefficient and $\tilde{n}_l = n_l - \sum_{i=0}^{l-1} \mu_{l,i} \tilde{n}_i$ as MP noise coefficient, then the decomposed signal at the reference sensor output can be written as

$$\mathbf{x} = \sum_{l=0}^{L-1} \tilde{c}_l \mathbf{g}_l + \sum_{l=0}^{L-1} \tilde{n}_l \mathbf{g}_l + \mathbf{x}^{[L]}.$$ (18)

It is evident from the above equations that the MP coefficient at each iteration includes both signal and noise coefficients, i.e., $\hat{c}_l = \tilde{c}_l + \tilde{n}_l$. We assume that the signal is properly decomposed by the L iterations and the remainder is only noise. Then, the decomposed first-sensor output is (subscript is returned)

$$\hat{\mathbf{x}}_1 = \sum_{l=0}^{L-1} \tilde{c}_l \mathbf{g}_l + \sum_{l=0}^{L-1} \tilde{n}_{1,l} \mathbf{g}_l \ . \tag{19a}$$

Using the same decomposition atoms, $\{\mathbf{g}_l\}$, for all other sensors, we obtain

$$\hat{\mathbf{x}}_m = \sum_{l=0}^{L-1} e^{j(m-1)\omega} \tilde{c}_l \mathbf{g}_l + \sum_{l=0}^{L-1} \tilde{n}_{m,l} \mathbf{g}_l ; \quad m = 2,3,...,M \ . \tag{19b}$$

Equivalently, the above expression can be represented as,

$$\hat{x}_m(t) = \sum_{l=0}^{L-1} e^{j(m-1)\omega} \tilde{c}_l g_l(t) + \sum_{l=0}^{L-1} \tilde{n}_{m,l} g_l(t) ; \quad m = 1,2,...,M \ . \tag{20}$$

Stacking the results for all the N antennas yields,

$$\hat{\mathbf{x}}(t) = \mathbf{a}(\theta) \tilde{\mathbf{c}} \mathbf{g}(t) + \tilde{\mathbf{N}} \mathbf{g}(t) \ , \tag{21}$$

where $\hat{\mathbf{x}}(t) = [\hat{x}_1(t), \hat{x}_2(t),...,\hat{x}_M(t)]^T$ is the decomposed array output, $\mathbf{a}(\theta) \in C^{M \times 1}$ is the steering vector,

$\tilde{\mathbf{c}} = [\tilde{c}_0, \tilde{c}_1,...,\tilde{c}_{L-1}] \in C^{1 \times L}$ is the MP signal coefficient vector, $\mathbf{g}(t) = [g_0(t), g_1(t),..g_{L-1}(t)]^T \in C^{L \times 1}$ includes the L

leading atoms, and $\tilde{\mathbf{N}} = [\tilde{\mathbf{n}}_1, \tilde{\mathbf{n}}_2,...,\tilde{\mathbf{n}}_M]^T \in C^{M \times L}$ is the noise matrix with $\tilde{\mathbf{n}}_m = [\tilde{n}_{m,0}, \tilde{n}_{m,1},...\tilde{n}_{m,L-1}]^T$.

Because atoms do not bear the DOA information, we only consider the MP decomposition coefficient matrix,

$$\hat{\mathbf{C}} = \mathbf{a}(\theta) \tilde{\mathbf{c}} + \tilde{\mathbf{N}}, \tag{22}$$

where $\hat{\mathbf{C}}$ is of size $M \times L$. The MP spatial correlation matrix, according to Eq. (22), is

$$\hat{\mathbf{C}} \hat{\mathbf{C}}^H = \mathbf{a}(\theta) \tilde{\mathbf{c}} \tilde{\mathbf{c}}^H \mathbf{a}^H(\theta) + \mathbf{a}(\theta) \tilde{\mathbf{c}} \tilde{\mathbf{N}}^H + \tilde{\mathbf{N}} \tilde{\mathbf{c}}^H \mathbf{a}^H(\theta) + \tilde{\mathbf{N}} \tilde{\mathbf{N}}^H \ . \tag{23}$$

Taking the expected value of both sides of the above equation, and applying the zero-mean property of the noise matrix, the MP coefficient covariance matrix is derived

$$E[\hat{\mathbf{C}} \hat{\mathbf{C}}^H] = \mathbf{a}(\theta) \tilde{\mathbf{c}} \tilde{\mathbf{c}}^H \mathbf{a}^H(\theta) + \tilde{\sigma}_n^2 \mathbf{I} \ . \tag{24}$$

For more details about the expression of $\tilde{\sigma}_n^2$, see Appendix B. The extension of Eq. (24) to multiple sources is straightforward and will involve the steering matrix $\mathbf{A}$. We maintain that, however, that most effective DOA estimation is achieved when dealing with each source separately.

5. PERFORMANCE ANALYSIS

5.1 SNR Analysis

In Section 3, we formulated the covariance matrix using MP coefficients. In this section, we focus on MP SNR improvement. The MP SNR improvement was demonstrated by simulations in [32]-[34] via the decomposition and reconstruction of the signal, but no analytic expressions were derived. We note that when considering, the narrowband arrays, the SNR enhancement for all sensor outputs are the same.

Suppose the signal is decomposed only one time, the MP coefficient is,

$$\hat{c}_0 = \tilde{c}_0 + \tilde{n}_0 . \tag{25}$$

As shown in Appendix B, the noise variance at the first iteration is $\tilde{\sigma}_n^2 = \sigma_n^2$. Therefore, the output SNR is:

$$\mathrm{SNR}_1 = \frac{|\tilde{c}_0|^2}{\sigma_n^2} . \tag{26}$$

If the first atom perfectly matches the signal, then the MP amounts to applying matched filtering where the output SNR depends on the signal energy. For two-time decomposition, the noise variance is $\tilde{\sigma}_n^2 = \sigma_n^2(2-|\mu_{1,0}|^2)$ and the average output SNR becomes

$$\mathrm{SNR}_2 = \frac{|\tilde{c}_0|^2 + |\tilde{c}_1|^2}{\sigma_n^2(2-|\mu_{1,0}|^2)} . \tag{27}$$

When more atoms are used, we invoke the approximations stated in Appendix B, Eqs. (B6) and (B7), regarding the atom cross-correlation values. In this case, the average output SNR at the end of L signal decompositions is

$$\mathrm{SNR}_L = \frac{\sum_{l=0}^{L-1}|\tilde{c}_l|^2}{\sigma_n^2(L-\sum_{l=1}^{L-1}\sum_{i=0}^{l-1}|\mu_{l,i}|^2)} . \tag{28}$$

Therefore, for signals with constant modulus over the entire T samples and is captured in L iterations of MP decomposition, the average output SNR can be expressed by,

$$\mathrm{SNR}_L = \frac{N\sigma_s^2}{\sigma_n^2(L-\sum_{l=1}^{L-1}\sum_{i=0}^{l-1}|\mu_{l,i}|^2)} , \tag{29}$$

where N is the number of snap shots. When the atoms are orthonormal, the double summation in Eq. (29) is negligible, and the SNR improvement using MP becomes N/L.

5.2 MP-MUSIC Performance Analysis

10

For the MUSIC algorithm, the asymptotic variance of the estimated spatial frequency is given for uncorrelated signals by [35]

$$\text{var}(\hat{\omega}_k) = \frac{1}{2N \cdot \Gamma_k \cdot h(\omega_k)} \left[1 + \frac{[(\mathbf{A}^H \mathbf{A})^{-1}]}{\Gamma_k} \right] , \tag{30}$$

where Γ_k is the input SNR of the k-th signal, $h(\omega_k) = \mathbf{d}^H(\omega_k)[\mathbf{I} - \mathbf{A}(\mathbf{A}^H \mathbf{A})^{-1}\mathbf{A}^H]\mathbf{d}^H(\omega_k)$, and $\mathbf{d}(\omega)$ is the derivative of the steering vector $\mathbf{a}(\theta)$ with respect to the spatial frequency ω. Specifically, when a single source is involved, the above expression becomes

$$\text{var}(\hat{\omega}_k) = \frac{6}{N \cdot \Gamma_k \cdot M \cdot (M^2 - 1)} \left[1 + \frac{1}{M \cdot \Gamma_k} \right] . \tag{31}$$

For MP-MUSIC that uses L coefficients from L iterations of MP decomposition to represent a single signal component, we can equivalent consider each MP coefficient as a data sample. As such, the above expression can be modified as

$$\text{var}(\hat{\omega}_k) = \frac{6}{L \cdot \text{SNR}_L \cdot M \cdot (M^2 - 1)} \left[1 + \frac{1}{M \cdot \text{SNR}_L} \right] . \tag{32}$$

To study the stop criterion in MP decomposition, let us consider that the $(L+1)$-th iteration yields an SNR of $\gamma_{L+1} = \eta \cdot \text{SNR}_L$. Typically, $0 < \eta \leq 1$, that is, including the $(L+1)$-th iteration would increase the number of iterations from L to $L+1$, but will lower the average SNR from SNR_L to approximately $\text{SNR}_L(L+\eta)/(L+1)$, yielding conflict contributions in the above expression. With straightforward computations, we can show that the MP-MUSIC performance is improved when the following condition is satisfied,

$$\eta \geq \frac{\sqrt{(M \cdot L \cdot \text{SNR}_L + 2L)^2 + 4L(1 + M \cdot \text{SNR}_L)} - (M \cdot L \cdot \text{SNR}_L + 2L)}{2(1 + M \cdot \text{SNR}_L)} . \tag{33}$$

Usually, the MP decomposition yields a high average SNR, i.e., $M \cdot \text{SNR}_L \gg 1$. In this case, the above expression can be approximated as $\eta \geq 1/(2 + M \cdot \text{SNR}_L)$ or, equivalently, $\gamma_{L+1} = \text{SNR}_L/(2 + M \cdot \text{SNR}_L) \approx 1/M$. As this sets a quite low hurdle, the inclusion of more iterations often leads to improved performance. On the other hand, at low SNR, i.e., $M \cdot \text{SNR}_L \ll 1$, the above condition becomes $\eta \geq 1/2$. That is, when the coefficients become very noisy, the decomposition should be terminated if the yielding SNR is lower than half of the average SNR of the previously decomposed coefficients. In practice, however, the MP decomposition should be terminated when the residue power is insignificant, or the operation becomes complicated, before the coefficients reach the low-SNR region.

6. SIMULATION RESULTS

We present different simulation examples to demonstrate the performance of MP-MUSIC for DOA estimation in comparison with TF-MUSIC and conventional MUSIC. Unless otherwise stated, we assume a uniform linear array of four sensors with an inter-sensor spacing of half wavelength. The noise is a zero-mean Gaussian white random process.

It is noted that the MP attempts to decompose a discrete time signal into a large number of atoms which are generated from a mother Gauusian function, with a pre-considered phase based on the dictionary type. The atoms are sampled in time to have the same length, N, as input signal or the residuals. In addition, the parameters that described an atom should also be discretized. In this paper, according to the length of observed signal snapshots, we discretize the parameter s, followed by the discretization of other variables, to generate the dictionary based on Gabor, chirplet, or cubic atoms. That is,

$s[j] = 2^j$, for $1 \le j \le J$, where $2^J \le N$.

$u = [0, N-1]$ where the step/increment value is $s[j]/2$.

$\zeta = [0, \pi]$ where the step/increment value is $\pi / s[j]$.

$\beta = [-\dfrac{\pi(s[j]-2)}{s^2[j]}, \dfrac{\pi(s[j]-2)}{s^2[j]}]$ where the step/increment value is $\pi / s^2[j]$.

$\xi = [-\dfrac{\pi(s[j]-2)}{10s^2[j]}, \dfrac{\pi(s[j]-2)}{10s^2[j]}]$ where the step/increment value is $\pi / 10s^2[j]$.

Example 1: Consider two sources with incident angles of $\pm 1.5°$ and the number of snapshot is $N=201$. The two sources emit closely separated parallel chirps, and the sum of their WVDs is shown in Fig. 1(a). When combined at the reference sensor, with 10 dB SNR, the WVD of the sum of the two chirps generates cross-terms which mask the auto-terms, as evident in Fig. 1(b). Although, it is difficult to separate auto-terms from cross-terms, we intentionally choose the highest 20 TF points that belongs to each chirp, as shown in Fig. 1(c). Selection of the source auto-term points should yield the best possible performance of STFD-based DOA estimation. We used two iterations involving two chirplet atoms, each captured one source signal. We then proceeded with the MUSIC technique applied to each coefficient separately. The spatial spectra of five independent trials with SNR=10dB for MUSIC, TF-MUSIC and

MP-MUSIC are shown in Fig. 2. For TF-MUSIC, the 20 TF auto-term points with highest energy concentration (shown in Fig. 1(c)) are used to construct the STFD matrix. Although we intentionally used the TF points correspond to auto-terms positions for each source separately, these points are nevertheless strongly affected by the cross-terms because of their close separations and, as such, prevent single-source DOA estimation. As a result, the TF-MUSIC, although performing DOA estimation separately for each source, yields estimated spatial spectra which show large estimation errors and are unable to clearly separate between the two sources.

Example 2: Consider two polynomial phase signals,

$$s_1(t) = \exp(j2\pi(0.317\,t\sin(0.002\,\pi t))), \quad s_2(t) = \exp(j2\pi(0.270\,t\sin(0.002\,\pi t)))\,. \tag{34}$$

The sum of the two individual signal WVDs is shown in Fig. 3(a). The incident source angles are $\pm 5^\circ$ and the number of snapshot is $N=231$. The WVD of the first sensor output, with SNR=0 dB, and the highest 20 TF points used by STFD are shown in Fig. 3(b). Notice that both types of cross-terms (inner and outer) exist in this plot. This makes the TFDs heavily cluttered and difficult to discriminate between signal components. However, the WVD suggests the presence of high-order polynomial phase type of signals. Therefore, we carried out the MP decomposition using two cubic atoms and performed DOA estimation for each atom separately. The auto-WVD [36] or MP distribution of the two cubic atoms are shown in Fig. 3(c). It is noted that if it is difficult to discern the appropriate set of atoms to use in MP, then one may perform spatial averaging of the WVDs across the sensor array [18], which is effective in reducing clutter by attenuating cross-terms and noise. The spatial spectra of five independent trials with SNR=0dB for MUSIC, TF-MUSIC and MP-MUSIC are shown in Fig. 4. Only the MP-MUSIC shows resolved DOA estimates.

Example 3: This example shows a case where the proper set of atoms is not known a priori or cannot be assumed. Consider the two signals depicted in Eq. (33) under exactly the same situations, i.e., incident source angles $\pm 5^\circ$, $N=231$, and SNR=0 dB. We now perform MP using six chirplets, rather than two cubic atoms. The WVD of each atom is shown in Fig. 5. The true signal IFs are also sketched in background. The spatial spectra of DOA estimation by using each coefficient separately are shown in Fig. 6(a), where the total root-mean-square error (RMSE) is equal to 2.036 degrees. In order to incorporate more atoms, i.e., more signal energy, in DOA estimation, we apply an association algorithm similar to that of [23]. In essence, we proceed as follows:

- Set the number of sources equal to the number of classes.

- Decompose the reference sensor output and use the same atoms for decompositions of other sensor outputs.

- Construct the MP coefficient covariance matrix at each iteration and determine the eigenvector that belongs to the largest eigenvalue. Denote the eigenvector for each iteration as $\mathbf{a}(u,\zeta)$.

- Given a set of vectors $\{\mathbf{a}(u_i,\zeta_i)\}$, we classify them into different classes $\{C_i\}$, each containing closely separated vectors. That is, $\mathbf{a}(u_i,\zeta_i)$ and $\mathbf{a}(u_j,\zeta_j)$ belong to the same class if $d(\mathbf{a}(u_i,\zeta_i),\mathbf{a}(u_j,\zeta_j)) < \varepsilon$, where ε is a properly chosen positive scalar. In this work, vector classification (association) is made according to their angles defined as

$$d(\mathbf{a}_i,\mathbf{a}_j) = \arccos(\tilde{\mathbf{a}}_i^T \tilde{\mathbf{a}}_j) . \tag{34}$$

where $\tilde{\mathbf{a}}_i = [\mathrm{Re}(\mathbf{a}_i)^T, \mathrm{Im}(\mathbf{a}_i)^T]^T$ and $\|\tilde{\mathbf{a}}_i\| = 1$. We select $\varepsilon = \pi/4$ as a predefined threshold for the case of two classes.

- Construct the MP coefficient covariance matrix for coefficients belong to the same class and estimate DOA.

The spatial spectra after atom classification or association are shown in Fig. 6(b). The RMSE is decreased to 1.15 degrees. It is clear from Fig. 5 that the 1st, 2nd, and 6th atoms belong to one source, whereas the 3rd and 5th atoms belong to the other source. However, the 4th atom captures parts of both sources. It is therefore expected that the DOA estimates will exhibit more bias when incorporating atom 4 into the array equations. When excluding atom 4, the DOA estimation results improve, as shown in Fig. 6(c), where the RMSE is 0.89 degree.

Example 4: Consider four source signals

$$s_k(t) = \exp(-\frac{(t - t_k)^2}{2\sigma^2}) \exp(j2\pi f_0(t - t_k)) ; k = 1,2,3,4 \tag{35}$$

where $f_0 = 5\,\mathrm{Hz}$, $\sigma^2 = 1$, $t_k = [30, 50, 60, 80]$, incident angles $\pm 5°$ and $\pm 10°$, number of snapshot $N=101$, and SNR=0 dB. The real part of the four signals is shown in Fig. 7. The sum of the individual signal WVD is shown in Fig. 8(a) that depicts signals burst with the same bandwidth. Since the number of sources is equal to the number of sensors, conventional MUSIC basically fails. In order to show the effect of a noisy atom on MP-MUSIC, we allow

the MP decomposition to include the fifth iteration. In this example, using either Gabor or chirplet dictionary nearly provided the similar performance. The auto-WVDs or MP distributions of the four leading Gabor atoms are shown in Fig. 8(b) and the WVD of the fifth Gabor atom is shown separately in Fig. 8(c). The magnitude of the coefficient corresponding to the fifth Gabor atom is considerably smaller than those belonging to the four leading atoms. There is a good match between the four atoms and the four signals, leaving the fifth atom coefficient with mainly noise, and consequently yielding an incorrect DOA estimate that is unassociated with any sources (see Fig. 9).

Example 5: This example is designed to evaluate Eqs. (B8) and (B9) that were derived for the noise variance at each iteration and the overall noise variance after L-iterations of MP decomposition. For this purpose, we consider the first component of the signal in Example 2, $s_1(t)$, and decompose the noise-free signal based on the chirplet dictionary. The number of iterations is set to 16. Because no noise is present, we consider the chosen atoms as the correct ones. Obviously some atoms may overlap in time, which means that $\mu_{l,l'}$ as we considered in Sections 4 and 5 is not zero. Now we consider the Gaussian random noise with zero mean and unit variance, $CN(0,1)$, which is decomposed using the same 16 atoms. The noise variance at each iteration and the overall noise variance after L iterations, obtained by averaging the results for 100 independent trials, are shown in Fig. 10 with red circle marks, whereas the results of Eqs. (B8) and (B9) are illustrated with black star marks. It is evident that the simulation results and analytically derived expressions coincide very well. In is also observed in Fig. 10 that the noise variance does not reduce rapidly with the number of iterations.

Example 6: In this example, we demonstrate how the MP-MUSIC performance varies as more iterations of MP decomposition are exploited. For simplicity and clarity of the illustration, we only use the first component of the signal used in Example 1, and the chirplet atoms are used. The RMSE performance averaged from 100 independent trials is shown in Fig. 11. Because the signal energy is concentrated in the first few iterations, the RMSE performance rapidly improves in these iterations. However, when the SNR is high, the RMSE performance generally continue to slowly decay as the number of iterations increases, whereas for low SNR, the RMSE performance may increase as more iterations are used. This observation generally coincides the discussion made in Section 5.

7. CONCLUSION

In this paper, we developed a high-resolution direction finding technique for nonstationary signals based on matching pursuit (MP). The MP decomposition coefficients bear the source angle information and are used to form a matrix congruent to the spatial covariance matrix. The direction-of-arrival (DOA) estimates are obtained from the subspace decomposition of the MP coefficient covariance matrix. The leading atoms of the MP, which capture most the source TF signatures, were shown to provide the desired source discrimination capability and enable DOA estimate of single sources. We provided signal-to-noise ratio (SNR) analysis of MP and validated the analytical expression by simulations. Simulation examples were presented which showed that the proposed MP-MUSIC outperforms the conventional MUSIC and TF-MUSIC. It was also shown that atoms which overlap with the signatures of two or more sources can cause bias in the estimates. Noisy atoms which remain after adequate representation of the signals should not be used, as they lead to incorrect estimates.

Appendix A

The additive noise at the output of sensors is considered with zero mean and temporally white, i.e., $E[n(t_1)n^*(t_2)] = \sigma_n^2 \delta(t_1 - t_2)$. Therefore, the random noise coefficient, n_l, is also zero mean

$$E[n_l] = E[<\mathbf{n}, \mathbf{g}_l>] = \sum_t E[n(t)]g_l^*(t) = 0 \tag{A1}$$

and with variance

$$E[n_l n_{l'}^*] = \sum_{t_1} \sum_{t_2} E[n(t_1)n^*(t_2)]g_{l'}(t_2)g_l^*(t_1) = \sigma_n^2 \mu_{l,l'}. \tag{A2}$$

Appendix B

The matrix $\widetilde{\mathbf{N}}\widetilde{\mathbf{N}}^H$ can be expressed as

$$\widetilde{\mathbf{N}}\widetilde{\mathbf{N}}^H = \begin{bmatrix} \widetilde{\mathbf{n}}_1^T \widetilde{\mathbf{n}}_1^* & \widetilde{\mathbf{n}}_1^T \widetilde{\mathbf{n}}_2^* & \ldots & \widetilde{\mathbf{n}}_1^T \widetilde{\mathbf{n}}_M^* \\ \widetilde{\mathbf{n}}_2^T \widetilde{\mathbf{n}}_1^* & \widetilde{\mathbf{n}}_2^T \widetilde{\mathbf{n}}_2^* & \ldots & \widetilde{\mathbf{n}}_2^T \widetilde{\mathbf{n}}_M^* \\ \vdots & \vdots & \vdots & \vdots \\ \widetilde{\mathbf{n}}_M^T \widetilde{\mathbf{n}}_1^* & \widetilde{\mathbf{n}}_M^T \widetilde{\mathbf{n}}_2^* & \ldots & \widetilde{\mathbf{n}}_M^T \widetilde{\mathbf{n}}_M^* \end{bmatrix} \tag{B1}$$

where $\tilde{\mathbf{n}}_m = [\tilde{n}_{m,0}, \tilde{n}_{m,1}, ... \tilde{n}_{m,L-1}]^T$. Because the sensor noise is assumed to be temporally and spatially white, the expectation value of $\tilde{\mathbf{N}}\tilde{\mathbf{N}}^H$ is a diagonal matrix with equal diagonal elements. As such, we focus on the m-th diagonal element, $E[\tilde{\mathbf{n}}_m^T \tilde{\mathbf{n}}_m^*]$, but drop the spatial subscript to simplify notation,

$$E[\tilde{\mathbf{n}}^T \tilde{\mathbf{n}}^*] = E[\tilde{n}_0 \tilde{n}_0^* + \tilde{n}_1 \tilde{n}_1^* + \cdots + \tilde{n}_{L-1} \tilde{n}_{L-1}^*]. \tag{B2}$$

The MP noise coefficient $\tilde{n}_l = n_l - \sum_{i=0}^{l-1} \mu_{l,i} \tilde{n}_i$ is determined recursively, where $\mu_{l,l'} = < \mathbf{g}_{l'}, \mathbf{g}_l >$ is the atom inner product or atom cross-correlation, and $\mu_{l,l'} \in [0,1]$. In order to compute the variance, we begin with the first decomposition,

$$E[\tilde{\mathbf{n}}^T \tilde{\mathbf{n}}^*] = E[\tilde{n}_0 \tilde{n}_0^*] = E[n_0 n_0^*] = \sigma_n^2. \tag{B3}$$

Therefore, $\tilde{\sigma}_n^2 = \sigma_n^2$. For two-time decompositions,

$$E[\tilde{\mathbf{n}}^T \tilde{\mathbf{n}}^*] = E[\tilde{n}_0 \tilde{n}_0^*] + E[\tilde{n}_1 \tilde{n}_1^*], \tag{B4}$$

where

$$E[\tilde{n}_1 \tilde{n}_1^*] = E[(n_1 - \mu_{1,0} n_0)(n_1 - \mu_{1,0} n_0)^*] = \sigma_n^2 (1 - |\mu_{1,0}|^2). \tag{B5}$$

Therefore, $\tilde{\sigma}_n^2 = \sigma_n^2 (2 - |\mu_{1,0}|^2)$. Because of the cross-correlation terms, a closed form expression for $\tilde{\sigma}_n^2$ becomes very complicated and does not necessarily help for insightful observations. In practice, however, atoms tend to assume small overlapping, and when the correlation of two atoms is raised to higher power or multiplied by another, the result is often negligible. Therefore, we make the following reasonable assumptions

$$\mu_{l,l'} \mu_{j,j'} = 0 \text{ ; if } l \neq l' \text{ or } j \neq j' \tag{B6}$$

and

$$|\mu_{l,l'}|^n = 0 \text{ ; if } n > 2. \tag{B7}$$

In this case,

$$E[\tilde{n}_l \tilde{n}_l^*] = \sigma_n^2 (1 - \sum_{i=0}^{l-1} |\mu_{l,i}|^2) \text{ ; } l \geq 1 \tag{B8}$$

and $E[\tilde{\mathbf{n}}^T \tilde{\mathbf{n}}^*] = \sum_{l=0}^{L-1} E[\tilde{n}_l \tilde{n}_l^*]$. As such,

$$\tilde{\sigma}_n^2 = \sigma_n^2 (L - \sum_{l=1}^{L-1} \sum_{i=0}^{l-1} | \mu_{l,i} |^2). \qquad\qquad (B9)$$

Notice that DOA estimation can be performed by using MP coefficients at each iteration separately, i.e., only considering coefficients that belong to an individual source. In this case, the noise variance is expressed in Eq. (B3) for the first iteration, and Eq. (B8) for the other iterations. As a result, when all atoms are orthogonal, the SNR for the l-th MP coefficient can be expressed as $| \tilde{c}_l |^2 / \sigma_n^2$.

REFERENCES

[1] A. Belouchrani and M. G. Amin, "Time-frequency MUSIC," IEEE Signal Processing Letters, vol. 6, no. 5, 1999, pp. 109-110.

[2] M. G. Amin, Y. Zhang, "Direction finding based on spatial time-frequency distribution matrices," Digital Signal Processing, vol. 10, no. 4, 2000, pp. 325-339.

[3] M. G. Amin, "Spatial time-frequency distributions for direction finding and blind source separation," SPIE Wavelet Conference, vol. 3723, 1999, pp. 62-70.

[4] A. Gershman and M. G. Amin, "Wideband direction-of-arrival estimation of multiple chirp signals using spatial time-frequency distributions," IEEE Signal Processing Letters, vol. 7, no. 6, 2000, pp. 152-155.

[5] M. G. Amin and A. Gershman, "High resolution sensor array processing in the presence of wideband chirps," Annual Asilomar Conference on Signals, Systems, and Computers, vol. 1, 2000, pp. 41-45.

[6] A. Gershman and M. G. Amin, "Coherent wideband DOA estimation of multiple FM signals using spatial time-frequency distributions," IEEE International Conference on Acoustics, Speech, and Signal Processing (ICASSP), vol. 5, 2000, pp. 3065-3068.

[7] L. Cohen, "Time-frequency distribution - A review," Proceedings of the IEEE, vol. 77, no. 7, 1989, pp. 941-980.

[8] R. O. Schmidt, "Multiple emitter location and signal parameter estimation," IEEE Trans. Antennas and Propagation, vol. AP-34, no. 3, 1986, pp. 276-280.

[9] B. Boashash, "Estimating and interpreting the instantaneous frequency of a signal- part 1: fundamental," Proceedings of IEEE, vol. 80, no. 4, 1992, pp. 520-538.

[10] S. G. Mallat and Z. Zhang, "Matching pursuit with time-frequency dictionaries," IEEE Trans. Signal Processing, vol. 41, no. 12, 1993, pp. 3397-3415.

[11] G. Z. Karabulut, T. Kurt and A. Yongacoglu, "Estimation of directions of arrivals by matching pursuit (EDAMP)," EURASIP Journal on Wireless Communications and Networking, 2005, pp. 197-205.

[12] S. F. Cotter, "Multiple snapshot matching pursuit for direction of arrival (DOA) estimation," 15th European Signal Processing Conference, 2007, pp. 247-251.

[13] G. Z. Karabulut, T. Kurt and A. Yongacoglu, "Angle of arrival detection by matching pursuit algorithm," 60th IEEE Vehicular Technology Conference, 2004, pp. 324-328.

[14] R. Sathish, "Improved direction-of-arrival estimation using wavelet based denoising techniques," Springer Journal of VLSI Signal Processing, 2006, pp. 29-48.

[15] M. A. Golroudbari and M.D. Allam, "Direction of arrival estimation in multipath environments using ICA and wavelet array denoising," 5th International Conference on Application of Information and Communication Technologies (AICT), 2011, pp. 1-5.

[16] Y. Xue, J. Wang and Z. Liu, "A novel improved MUSIC algorithm by wavelet denoising in spatially correlated noises," IEEE International Symposium on Communications and Information Technology (ISCIT), 2005, pp. 515-518.

[17] S. Xianglan and H. S. Ping, "Improvement of DOA estimation using wavelet denoising," International Conference on Information Science and Engineering (ICISE), 2009, pp. 587-590.

[18] W. Mu, M. G. Amin, and Y. Zhang, "Bilinear signal synthesis in array processing," IEEE Trans. Signal Processing, vol. 51, no. 1, 2003, pp. 90-100.

[19] S. Mann and S. Haykin, "The chirplet transform: physical considerations," IEEE Trans. Signal Processing, vol. 43, 1995, pp. 2745-2761.

[20] S. Ghofrani, D.C. McLernon and A. Ayatollahi, "Conditional spectral moments in matching pursuit based on the chirplet elementary function," Digital Signal Processing, vol. 18, 2008, pp. 694-708.

[21] A. Bultan, "A four-parameter atomic decomposition of chirplets," IEEE Trans. Signal Processing, vol. 47, no. 3, 1999, pp. 731-745.

[22] J. Cui and W. Wong, "The adaptive chirplet transform and visual evoked potentials," IEEE Trans. Biomedical Engineering, vol. 53, no. 7, 2006, pp. 1378-1384.

[23] L. T. Nguyen, A. Belouchrani, K. Abed-Meraim, and B. Boashash, "Separating more sources than sensors using time-frequency distributions," International Symposium on Signal Processing and its Application (ISSPA), 2001, pp. 583-586.

[24] A. Belouchrani and M. G. Amin, "Blind source separation based on time frequency signal representation," IEEE Trans. Signal Processing, vol. 46, no. 11, 1998, pp. 2888-2897.

[25] Y. Zhang and M. G. Amin, "Spatial averaging of time frequency distributions for signal recovery in uniform linear array," IEEE Trans. Signal Processing, vol. 48, no. 10, 2000, pp. 2892-2902.

[26] K. Sekihara, S. Nagarajan, D. Poeppel and Y. Miyashita, "Time frequency MEG-MUSIC algorithm," IEEE Trans. Medical Imaging, 18 (1), 1999, pp. 92-97.

[27] Z. Hong and and B. Zheng, "An efficient algorithm for adaptive chirplet-based signal decomposition," 5th IEEE International Conference on Signal Processing (ICSP), 2000, pp. 366-368.

[28] Q. Yin, S. Qian and A. Fenga, "Fast refinement for adaptive Gaussian chirplet decomposition," IEEE Trans. Signal Processing, vol. 50, no. 6, 2002, pp. 1298-1306.

[29] Y. Lu, R. Demirli, G. Cardoso and J. Saniie, "A successive parameter estimation algorithm for chirplet signal decomposition," IEEE Trans. Ultrasonics, Ferroelectrics and Frequency Control, vol. 53, no. 11, 2006, pp. 2121-2131.

[30] W. Yong and J. Yicheng, "Modified adaptive chirplet decomposition and its efficient implementation," 8th International Conference on Signal Processing (ICSP), 2006.

[31] S. Orr, "The order of computation for finite discrete Gabor transforms," IEEE Trans. Signal Processing, vol. 41, no. 1, 1993, pp. 122-130.

[32] G. Xu and J. Gao, "A new method of weak signal detection based on improved matching pursuit algorithm," IEEE International Joint Conference on Neural Networks and Computational Networks and Computational Intelligence, 2008, pp. 538-542.

[33] N. Ruiz-Reyes, P. Vera-Candeas, J. Curpian-Alonso, R. Mata-Campos, and J. C. Cuevas-Martinez, "New matching pursuit-based algorithm for SNR improvement in ultrasonic NDT," NDT&E International, vol. 38, 2005, pp. 453-458.

[34] N. Ruiz, P. Vera, J. Curpian, D. Martinez, and R. Mata, "Matching pursuit-based signal processing method to improve ultrasonic flaw detection in NDT application," IET Journals & Magazines, 20th Electronics Letters, vol.

39, no. 4, 2003, pp. 413-414.

[35] P. Stoica and A. Nehorai, "MUSIC, maximum likelihood, and Cramer-Rao bound," IEEE Trans. Signal Processing, vol. 37, no. 5, 1989, pp. 720-741.

[36] S. Ghofrani and D. C. McLernon, "Auto Wigner-Ville distribution via non adaptive and adaptive signal decomposition," Signal Processing, vol. 89, 2009, pp. 1540-1549.
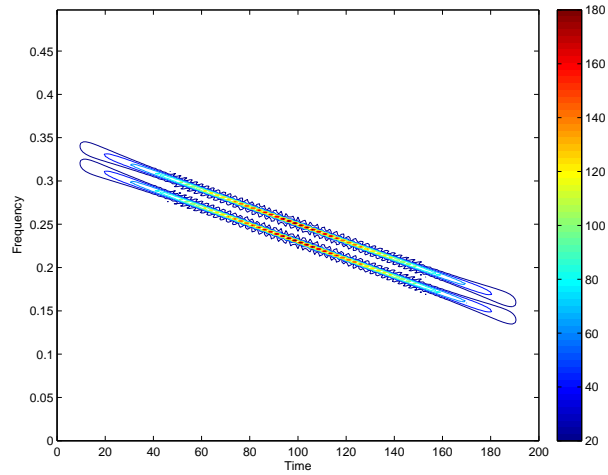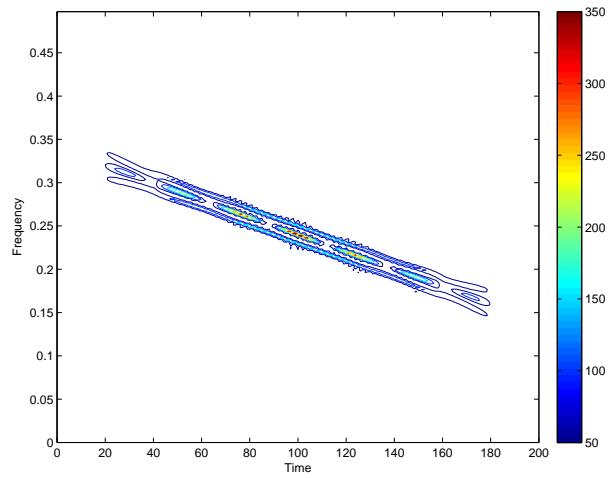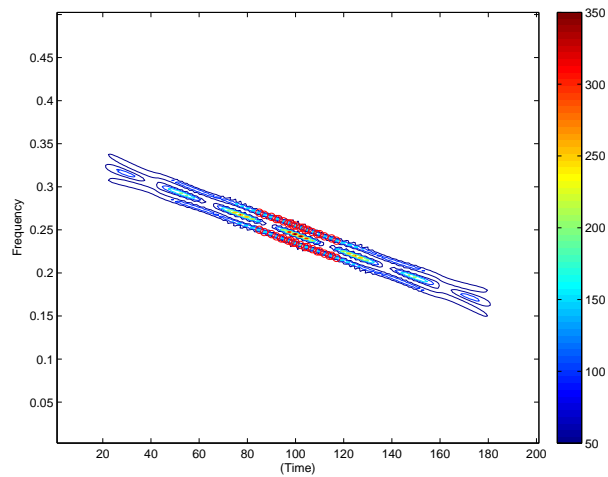
Fig. 1: (a) WVD of two parallel chirps which is computed individually and illustrated jointly, (b) WVD of the first

sensor output with SNR=10dB, and (c) 20 TF points located on chirps and used for STFD.
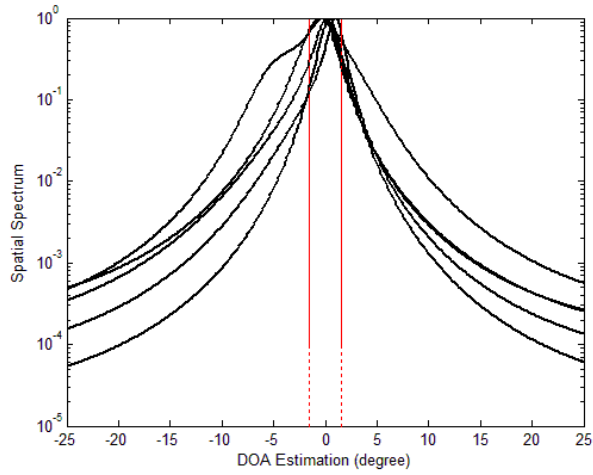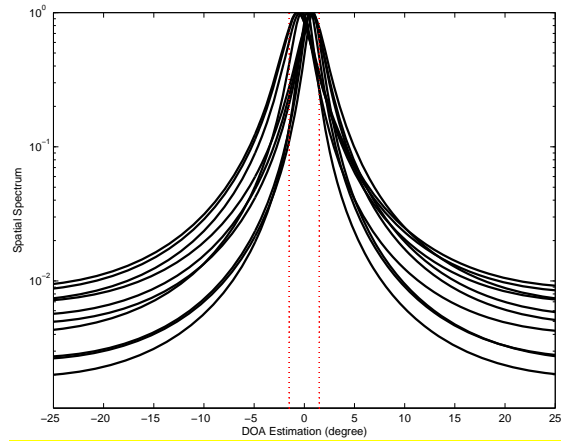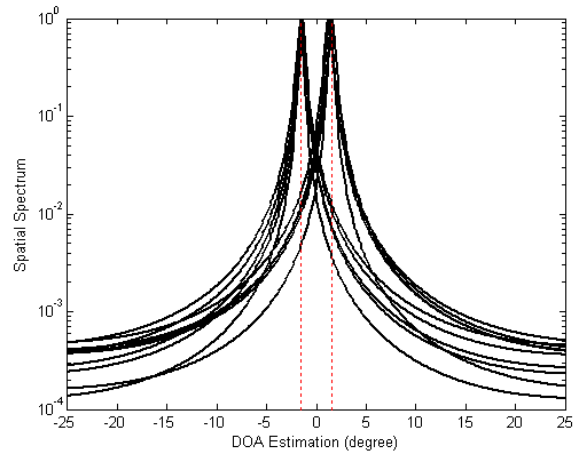
Fig. 2: Spatial spectra of five independent trials for two parallel chirps with close impinging angles of $\pm 1.5°$ and SNR=10dB (M=4, N=201). (a) MUSIC (b) TF-MUSIC using 20 maximum TF points for each source, and (c) MP-MUSIC based on chirplet atoms.
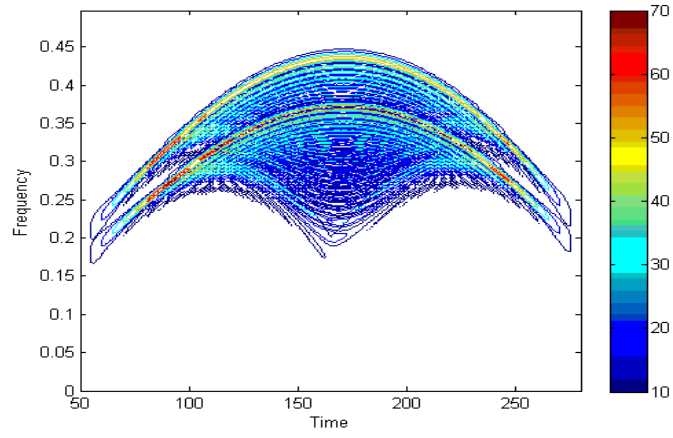
(a)
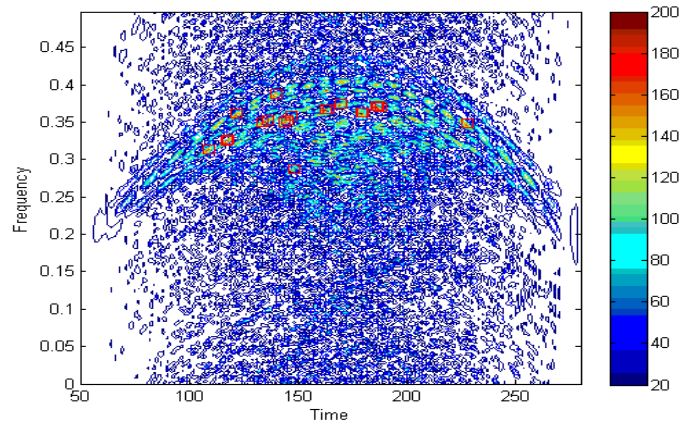
(b)
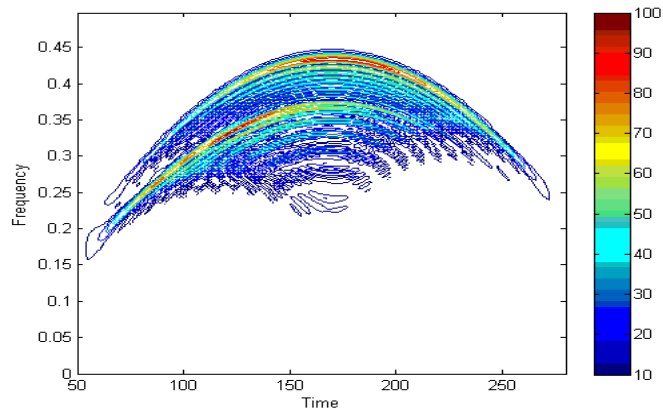
(c)

Fig. 3: (a) WVD of two close polynomial phase signal which is computed individually and illustrated jointly, (b) WVD of the first sensor output with SNR=0dB and 20 TF points, marked in red square, which are chosen based on finding peaks through in WVD, i.e. $f_i(t) = \arg\{\max_f(\mathbf{WV}(t, f))\}$, and (c) the MP distribution of two cubic chosen atoms with SNR=0dB.
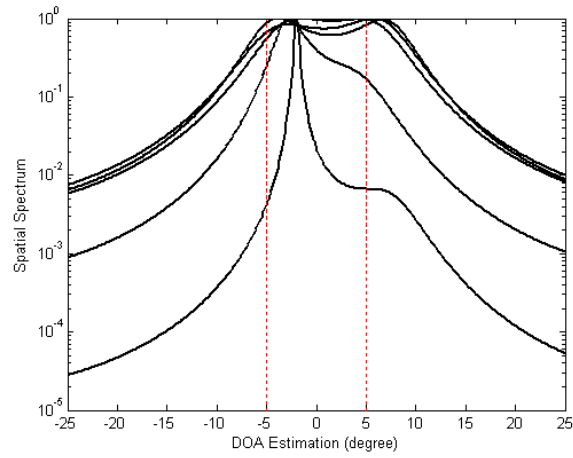
(a)
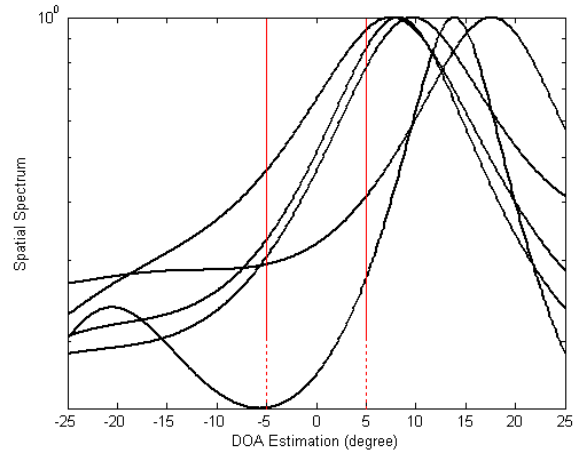
(b)
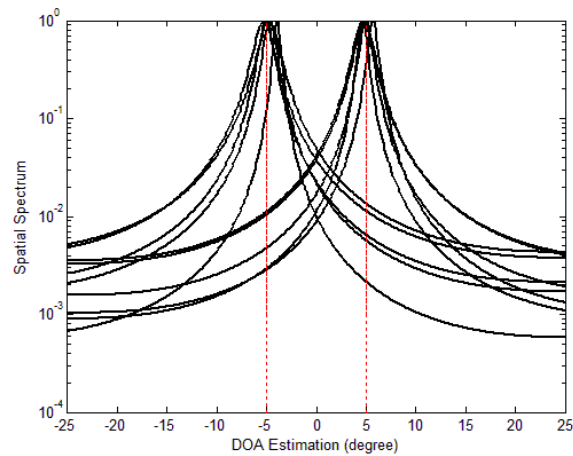
(c)

Fig. 4: Two polynomial phase sources with impinging angles, $\pm 5^{\circ}$, SNR=0dB, M=4, N=231. Estimated DOA for 5 independent trials by (a) MUSIC, (b) TF-MUSIC and (c) MP-MUSIC based on cubic atoms.
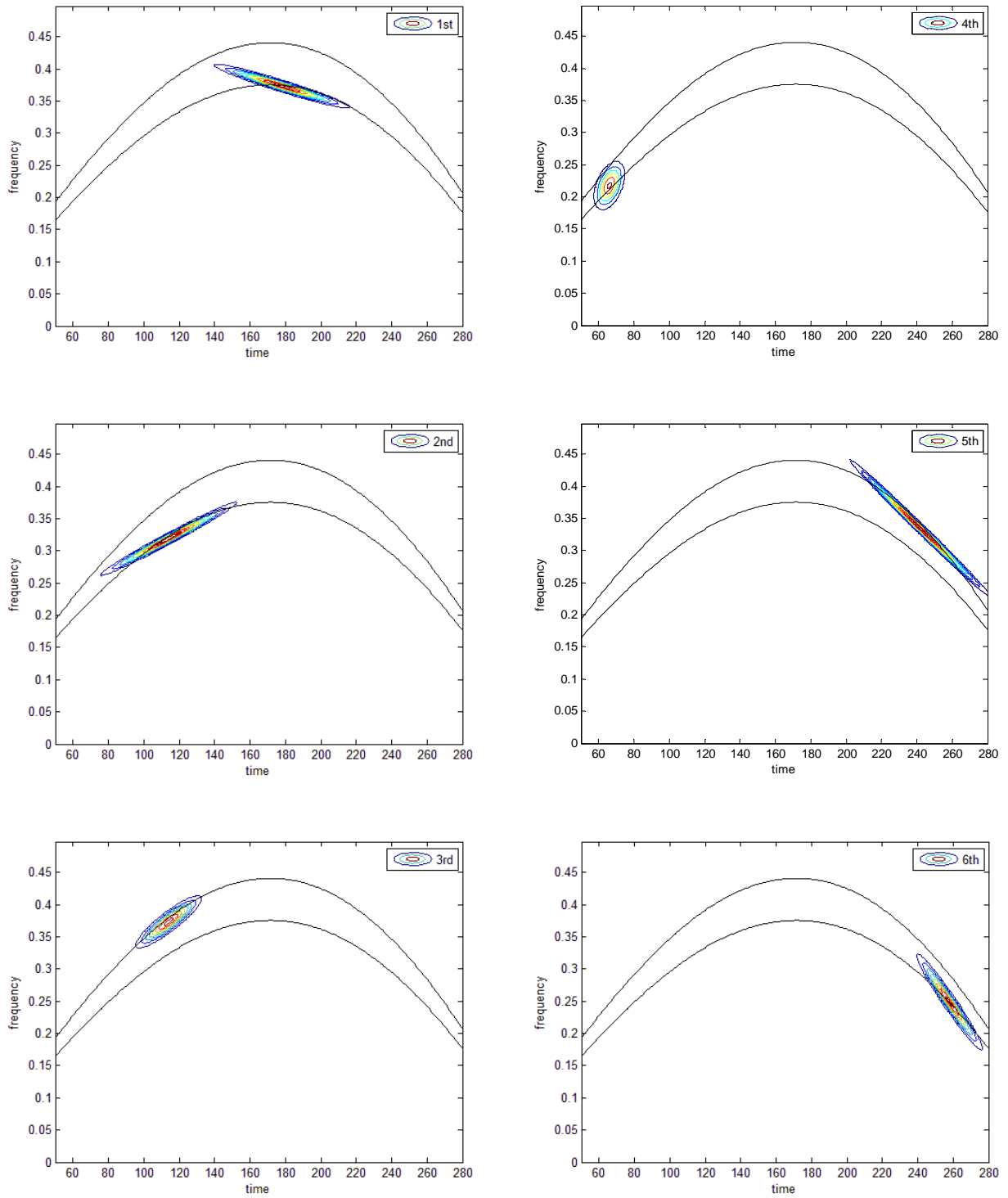
Fig. 5: WVD of six chirplet chosen atoms when the reference sensor output with SNR=0dB is decomposed.
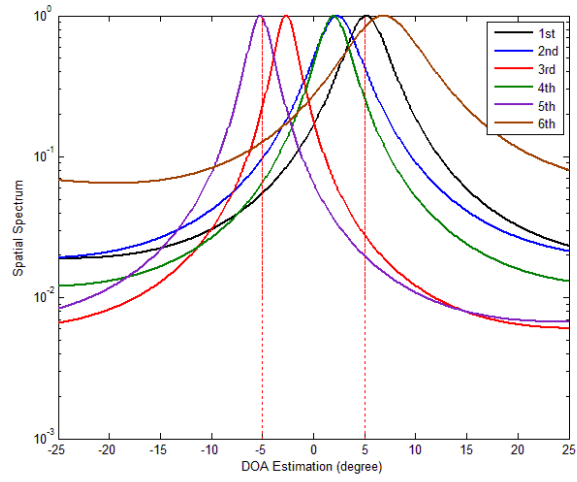
(a)
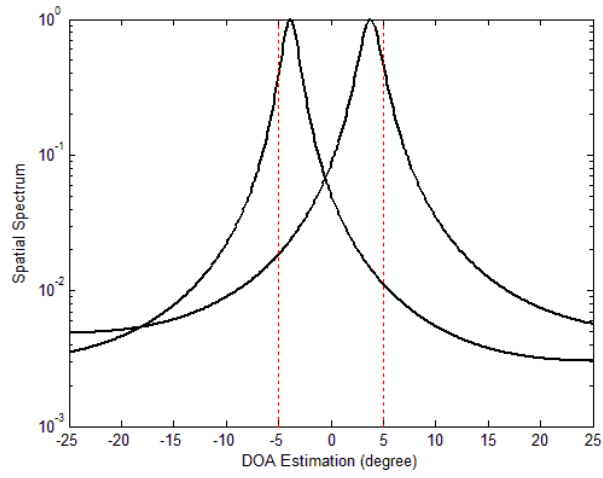
(b)
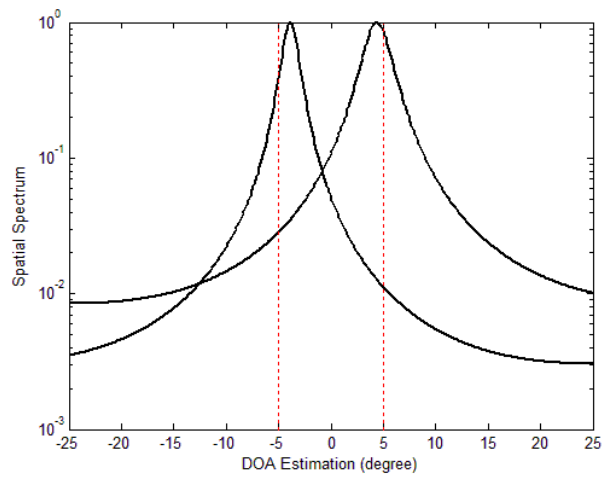
(c)

Fig. 6: Spatial spectra when performing DOA estimation (a) separately for each MP coefficient, (b) and (c) separately for each group.
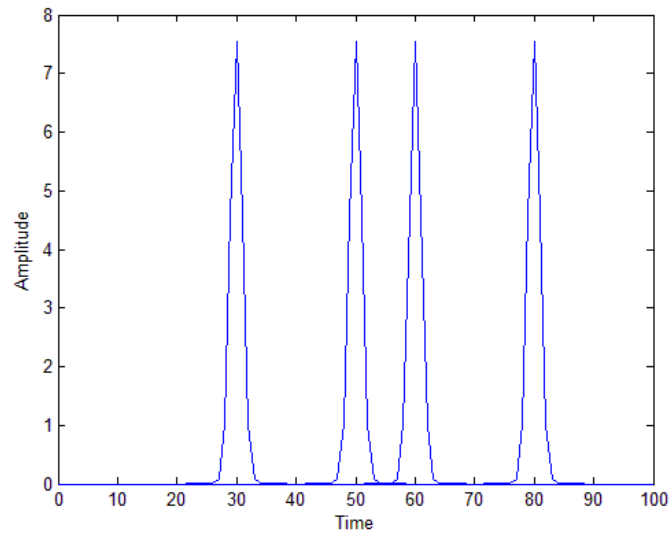
Fig. 7: The real part of four burst signals.
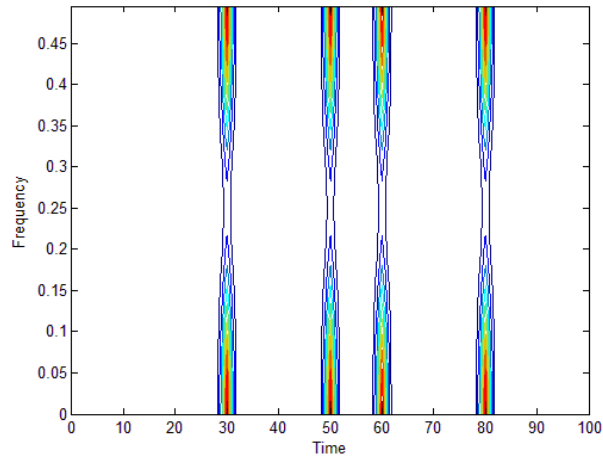
(a)
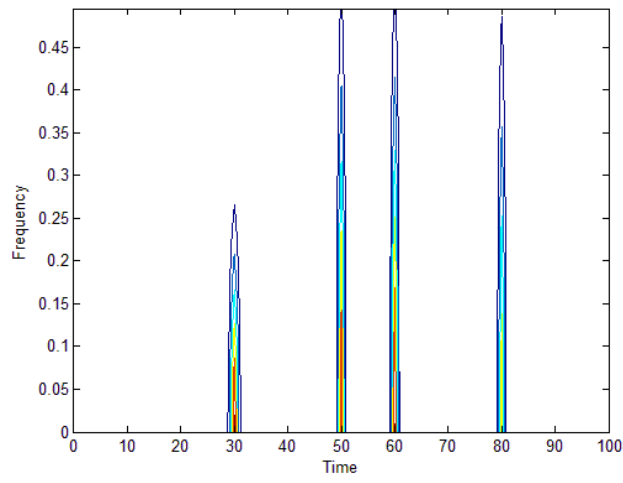
(b)
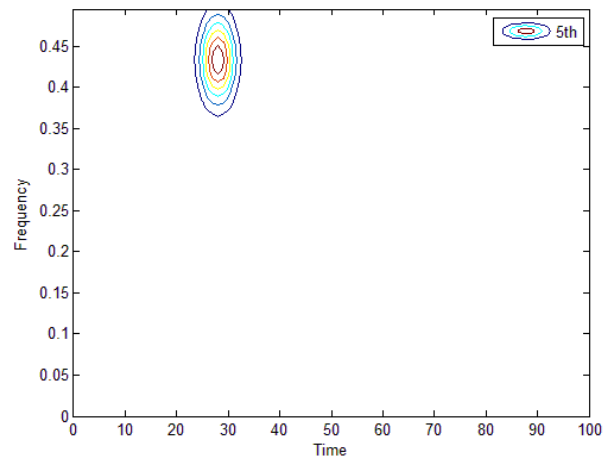
(c)

Fig. 8: (a) WVD of four burst signal with the same bandwidth which is computed individually and illustrated jointly,

(b) the MP distribution of four Gabor atoms, and (c) WVD of 5-th Gabor atom.
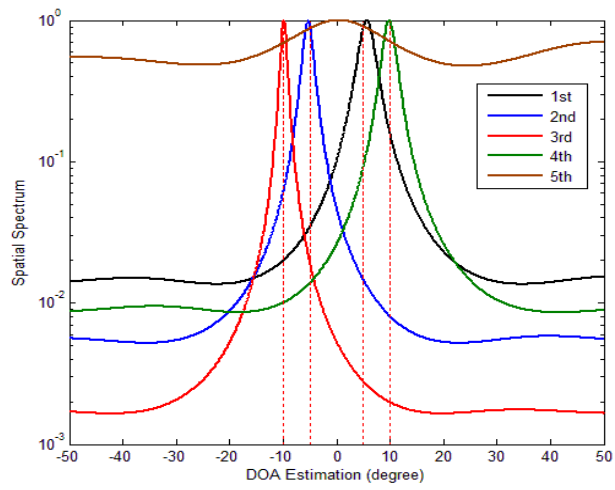
Fig. 9: Estimated DOA by five MP coefficients separately.
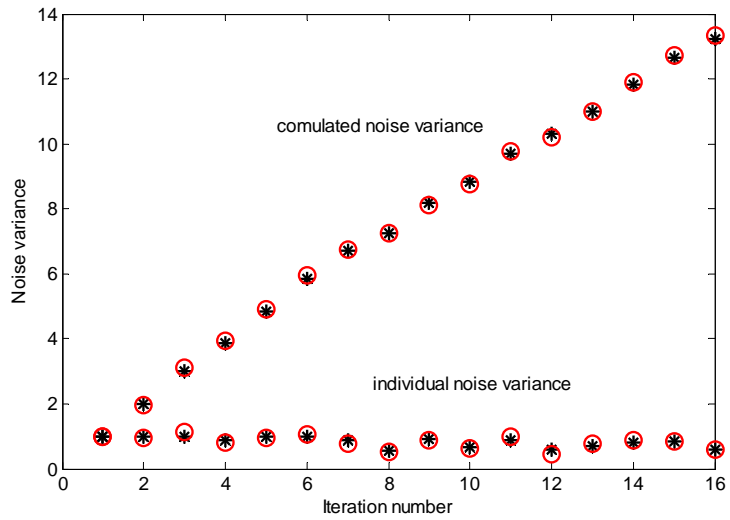
Fig. 10: Noise variance in each iteration and the accumulated noise variance computed analytically (black star) and by simulation (red circle).
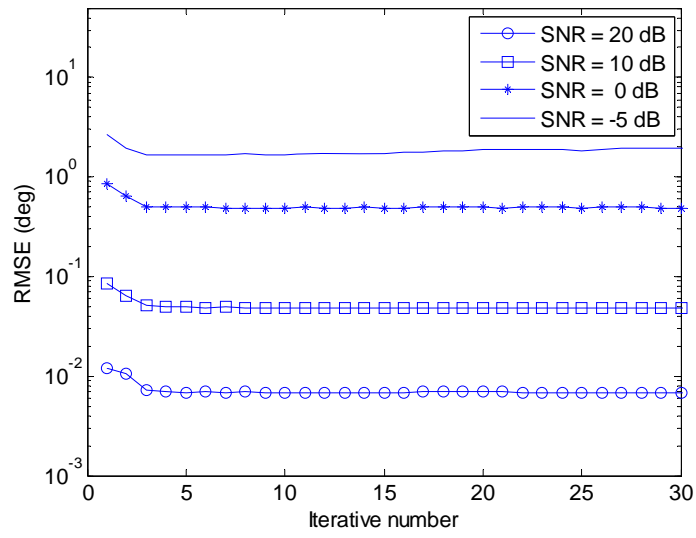
Fig. 11: The RMSE for MP-MUSIC based on chirplet dictionary.